Kynurenine 3-Monooxygenase from *Pseudomonas fluorescens*: Substrate-like Inhibitors both Stimulate Flavin Reduction and Stabilize the Flavin−Peroxo Intermediate yet Result in the Production of Hydrogen Peroxide

Karen R. Crozier-Reabe,[‡] Robert S. Phillips,[§] and Graham R. Moran*[,‡]

Department of Chemistry and Biochemistry, University of Wisconsin, 3210 North Cramer Street, Milwaukee, Wisconsin 53211-3029, and Departments of Chemistry and of Biochemistry and Molecular Biology, University of Georgia, Athens, Georgia 30602-2556

Received June 3, 2008; Revised Manuscript Received September 10, 2008

ABSTRACT: Kynurenine 3-monooxygenase (KMO) is a flavin-dependent hydroxylase that catalyzes the conversion of L-kynurenine (L-Kyn) to 3-hydroxykynurenine (3OHKyn) in the pathway for tryptophan catabolism. KMO inhibition has been widely suggested as an early treatment for stroke and other neurological disorders that involve ischemia. We have investigated the reductive and the oxidative half-reactions of a stable form of KMO from *Pseudomonas fluorescens* (*KMO*). The binding of L-Kyn by the enzyme is relatively slow and involves at least two reversible steps. The rate constant for reduction of the flavin cofactor by NADPH increases by a factor of $\sim 2.5 \times 10^3$ when L-Kyn is bound. The rate of reduction of the KMO•L-Kyn complex is 160 s^{-1}, and the K_d for the NADPH complex is 200 μM with charge-transfer absorption bands for the KMO_{RED}•L-Kyn•$NADP^+$ complex accumulating after reduction. The reduction potential of *KMO* is −188 mV and is unresponsive to the addition of L-Kyn or other inhibitory ligands. KMO inhibitors whose structures are reminiscent of L-Kyn such as *m*-nitrobenzoylalanine and benzoylalanine also stimulate reduction of flavin by NADPH and, in the presence of dioxygen, result in the stoichiometric liberation of hydrogen peroxide, diminishing the perceived therapeutic potential of inhibitors of this type. In the presence of the native substrate, the oxidative half-reaction exhibits triphasic absorbance data. A spectrum consistent with that of a peroxyflavin species accumulates and then decays to yield the oxidized enzyme. This species then undergoes minor spectral changes that, based on flavin difference spectra defined in the presence of 3OHKyn, can be correlated with product release. The oxidative half-reaction observed in the presence of saturating benzoylalanine or *m*-nitrobenzoylalanine also shows the accumulation of a peroxyflavin species that then decays to yield hydrogen peroxide without hydroxylation.

Kynurenine 3-monooxygenase (KMO)[1] is an external flavoprotein aromatic hydroxylase (FAH) that catalyzes the hydroxylation of L-kynurenine (L-Kyn) to form 3-hydroxykynurenine (3OHKyn) (Scheme 1). This activity is central to tryptophan degradation that in higher organisms leads to the production of nicotinamide adenine dinucleotide (*1*). There has been sustained interest in KMO because it has been deemed a potential therapeutic target for limiting neuronal damage during ischemic events such as stroke and seizures (*2, 3*). At least one KMO inhibitor is in preclinical trials for the treatment of Huntington's disease (Ro618048 in Scheme 2) (*4*).

Neuron death during and after a hypoxic event is caused by an elevated local concentration of the neurotransmitter glutamate, which binds at *N*-methyl D-aspartate (NMDA) receptors promoting calcium influx, leading to hyperstimulation and subsequent cellular death. KMO has a role in defining the balance of NMDA receptor agonists and antagonists as the reaction that is catalyzed leads directly to the production of the NMDA receptor agonist, quinolinate, and the apoptotic signals, 3OHKyn and xanthurenate (*5*) (Scheme 3). Therefore, KMO inhibition will halt the production of these apparently detrimental molecules and force the accumulation of L-Kyn. L-Kyn, however, is also a substrate for two other enzymes, kynurenine aminotransferase (KAT) and kynureninase. KAT catalyzes the reaction of L-Kyn to the NMDA receptor antagonist, kynurenate. Not only does kynurenate block glutamate activity at the receptor but it also has the reported capacity to suppress glutamate release (*6*). Therefore, inhibition of KMO has the synergistic neuroprotective effects of halting glutamate release, suppressing its activity at NMDA receptors, and minimizing the accumulation of specific neurotoxic and/or apoptotic metabolites. A

* To whom correspondence should be addressed: Department of Chemistry and Biochemistry, University of Wisconsin, 3210 N. Cramer St., Milwaukee, WI 53211-3029. Telephone: (414) 229-5031. Fax: (414) 229-5530. E-mail: moran@uwm.edu.

‡ University of Wisconsin.

§ University of Georgia.

[1] Abbreviations: KMO, kynurenine 3-monooxygenase; L-Kyn, L-kynurenine; 3OHKyn, 3-hydroxykynurenine; FAH, flavoprotein aromatic hydroxylase; KAT, kynurenine aminotransferase; DTT, dithiothreitol; NMDA, *N*-methyl-D-aspartate; BA, benzoylalanine; *m*-NBA, *m*-nitrobenzoylalanine; HP, 1-hydroxyphenazine; HEPES, *N*-(2-hydroxyethyl)piperazine-*N*′-2-ethanesulfonic acid; FAD, flavin adenine dinucleotide; NADPH, nicotinamide adenine dinucleotide phosphate; PHBH, *p*-hydroxybenzoate hydroxylase; PHHY, phenol hydroxylase; MHBH, *m*-hydroxybenzoate hydroxylase.

10.1021/bi8010434 CCC: $40.75
Published on Web 10/28/2008

Scheme 1

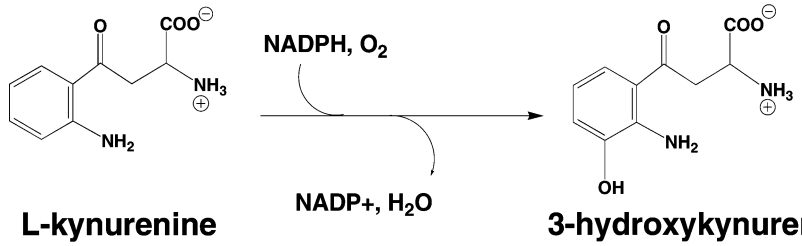

Scheme 2

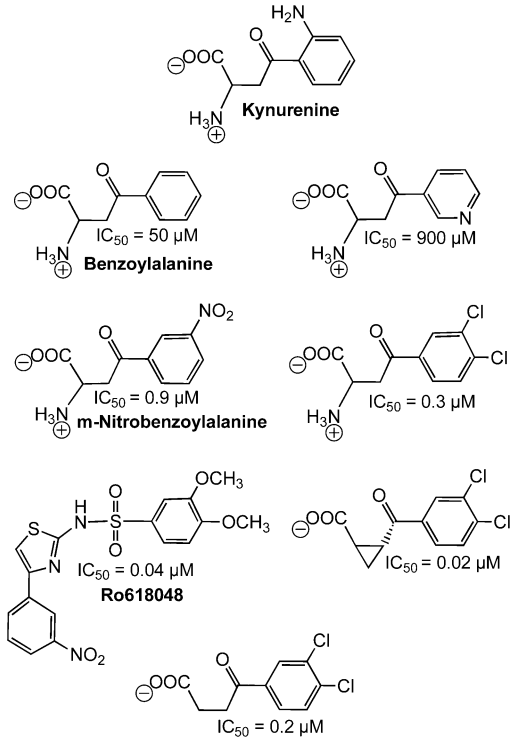

number of inhibitors that have been designed to target KMO mimic the structure of L-Kyn (Scheme 2). The inherent disadvantage with this approach is that such molecules also tend to inhibit KAT to some extent (*2, 7*), resulting in a decreased level of accumulation of the potentially beneficial metabolite, kynurenate (*8, 9*).

KMO is a little-known FAH enzyme that, based on its primary structure, is categorized as a class A flavoprotein hydroxylase (*10*). All class A FAHs are single-component enzymes that have a tightly bound FAD cofactor, hydroxylate exclusively activated aromatic substrates, reduce molecular oxygen by four electrons, and require reduced pyridine nucleotide phosphate (*11*). The paradigm examples within this enzyme group are *p*-hydroxybenzoate hydroxylase (PHBH) (*12*) and phenol hydroxylase (PHHY), of which the reaction mechanisms are known in exquisite detail. The extent of the understanding of the chemistry is largely due to the spectrophotometric reporting power of the FAD cofactor and the fact that the catalytic mechanism can be conveniently studied as separate reductive and oxidative half-reactions.

For the class A FAH enzymes, the aromatic substrate binds and stimulates the rate at which the flavin isoalloxazine ring is reduced by NADPH by multiple orders of magnitude (*13*−*15*). This couples aromatic substrate acquisition to hydride transfer and ultimately hydroxylation, preventing reduction of the flavin in the absence of the aromatic substrate that, in these enzymes, results in the loss of reducing equivalents in the formation of hydrogen peroxide during reoxidation of the FAD cofactor. In the oxidative half-reaction, the reduced enzyme−aromatic substrate complex reacts with dioxygen and three flavin−oxo intermediates can be observed to form before the release of the hydroxylated product (*16, 17*). The two half-reactions have been found to be dependent on the movement of the flavin isoalloxazine into and out of the active site. The enzymes are thought to have three positions for the isoalloxazine ring that are used to gate access and release of substrates and products and sequester key catalytic steps from the solvent (*18*).

KMO is one of the few FAH enzymes found in higher organisms; however, KMOs from these sources have proven to be difficult to purify and study due to marked instability (*19, 20*). A number of bacteria harbor select activities of tryptophan catabolism, including that of KMO (*21*). At least one of these forms of KMO, that from *Pseudomonas fluorescens,* has been shown to be sufficiently stable to be expressed heterologously and isolated (*22*). In this investigation, we examine substrate acquisition and the reductive and oxidative half-reactions of KMO from *P. fluorescens*.

MATERIALS AND METHODS

Materials. FAD, L-Kyn, and HEPES buffer were each purchased from ACROS. NADPH and *m*-nitrobenzoylalanine (*m*-NBA) were purchased from Alexis. 1-Hydroxyphenazine (HP) was purchased from TCI America. Dithiothreitol (DTT), xanthine, xanthine oxidase, methyl viologen, and catalase were from Sigma-Aldrich. Benzoylalanine (BA) was synthesized according to published protocols (*23*).

Preparation and Assay of Kynurenine 3-Monooxygenase. KMO was expressed and purified according to previously published methods (*22*). Low concentrations of sodium chloride were observed to stabilize the enzyme during the experimentation, and unless stated otherwise, 10 mM NaCl was added to enzyme samples. Enzyme assays were conducted on a Hansetech oxygen electrode to monitor the change in dioxygen concentration with time. Routine enzyme assays were conducted in 20 mM HEPES and 2 mM DTT (pH 7.5), in the presence of 500 μM L-Kyn, 500 μM NADPH, and atmospheric oxygen ($\sim$250 μM) at 25 °C. The initial rate of reactions was measured within the first 40 s of turnover.

Substrate Binding to Oxidized KMO. The kinetics of binding of the native substrate, L-Kyn, to oxidized KMO were monitored at 450 nm using a Hi-Tech Scientific DX2 stopped-flow spectrophotometer. A reaction mixture of aerobic 80 μM KMO and 4 mM DTT was mixed with various pseudo-first-order concentrations of aerobic L-Kyn

Scheme 3

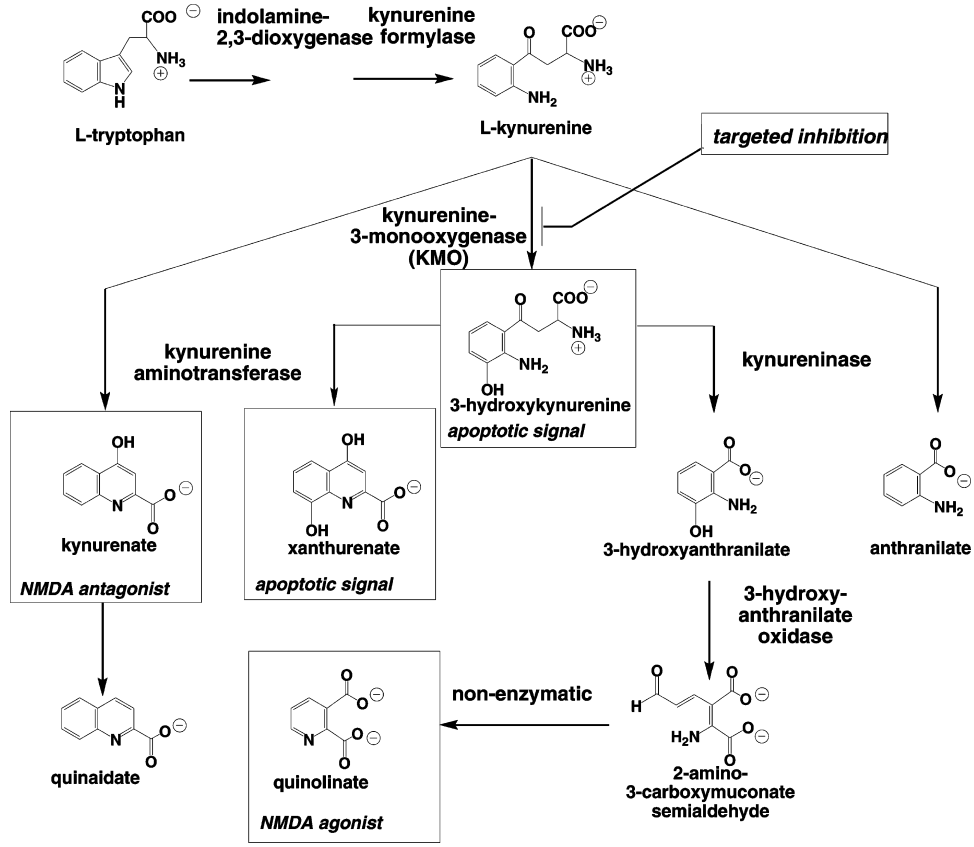

(final concentrations of 0.4−2.2 mM) at 5 °C. Each absorbance trace was fit to a sum of two exponentials, and the rate constants associated with the first phase, k_1, were plotted against L-Kyn concentration to determine the association and dissociation rate constants associated with this initial binding event.

Reduction Potential Measurements. Reduction potentials were measured for unliganded KMO and the KMO·L-Kyn, KMO·*m*-NBA, and KMO·BA complexes at 5 °C using the xanthine/xanthine oxidase reduction system of Massey (*24*). A Hewlett-Packard 8453 diode-array spectrophotometer was used to monitor the reduction of the enzyme in the presence of a dye of known potential. The reaction mixture was placed in an anaerobic cuvette and consisted of 300 μM xanthine, 5 μM methyl viologen, 10 μM 1-hydroxyphenazine (HP), 10 μM *KMO*, and a saturating ligand concentration (if required) (*22*) in 20 mM HEPES buffer (pH 7.5) at 5 °C. Once the mixture was made anaerobic by 45 cycles of argon and vacuum at 5 °C, xanthine oxidase (final concentration of 1−2 μM) was added from a sidearm to initiate the reduction of the enzyme and dye. Spectra were recorded every 5 min until no further spectral changes were observed. The data were analyzed according to eqs 1−4. Equations 1 and 2 were used to obtain the fraction of reduced and oxidized KMO at 480 nm, where the dye has no contribution. Equations 3 and 4 were used similarly to obtain the fraction of reduced and oxidized HP at 370 nm but include subtraction of the contribution of the enzyme cofactor based both on the extinction coefficient change for the enzyme bound FAD at this wavelength ($\Delta\varepsilon_{KMO}$) and on the fraction of enzyme reduced as ascertained from the 480 nm data. The log of the ratio of the oxidized and reduced forms of HP was then plotted against the log of the same ratio for KMO, and the HP midpoint was substituted into the Nernst equation to yield the reduction potential, where A is the absorbance, A_i is the initial absorbance, A_f is the final absorbance, and F is the fraction of species.

$$F(\mathrm{KMO_{OX}}) = (A - A_f)/(A_i - A_f) \quad (1)$$

$$\log(\mathrm{KMO_{OX}})/(\mathrm{KMO_{RED}}) = \log[F(\mathrm{KMO_{OX}})]/[1 - F(\mathrm{KMO_{OX}})] \quad (2)$$

$$F(\mathrm{HP_{OX}}) = [A - \Delta\varepsilon_{KMO}\cdot[\mathrm{KMO}]\cdot F(\mathrm{KMO_{OX}}) - A_f]/(A_i - A_f) \quad (3)$$

$$\log(\mathrm{HP_{OX}})/(\mathrm{HP_{RED}}) = \log[F(\mathrm{HP_{OX}})]/[1 - F(\mathrm{HP_{OX}})] \quad (4)$$

Measurement of the K_d for the KMO_{RED}·L-Kyn Complex. Spectrophotometric measurement of the constant for dissociation of the KMO_{RED}·L-Kyn complex to the reduced enzyme was attempted by monitoring the spectrum of the reduced enzyme when it was titrated with L-Kyn. A gastight Hamilton syringe with a threaded plunger was adapted via a ground glass fitting to an anaerobic cuvette equipped with two sidearms. A mixture of 10 μM KMO, 300 μM xanthine, 5 μM methyl viologen, and 2 mM glucose in 20 mM HEPES buffer (pH 7.5) was added to the body of the cuvette. Xanthine oxidase (final concentration of 500 nM) and 25 units of glucose oxidase were then added to individual side arms. A 5.2 mM L-Kyn sample with 5 mM glucose was sparged for 10 min with argon and drawn into the gastight syringe preloaded with 50 units of glucose oxidase. The syringe was fitted to the cuvette, and the entire apparatus was made anaerobic with 45 cycles of vacuum and argon at 5 °C. Once the mixture had become anaerobic, xanthine

oxidase was added from a sidearm to reduce KMO (*24*). Glucose oxidase was then added from the second sidearm to ensure anaerobic conditions were maintained throughout the experiment. L-Kyn was then titrated (from 0 to 300 μM) to KMO_{RED} at 5 °C. The sample was left to equilibrate for 30 min between each addition, and spectra were recorded using a Varian Cary 3 UV−vis spectrophotometer equipped with a thermostated cuvette holder. The sample cavity of the spectrophotometer was flushed with nitrogen gas to eliminate condensation.

Stopped-Flow Measurements of the Reductive Half-Reaction of KMO. The limiting rate of reduction of the flavin cofactor, the dissociation constant for NADPH, and the rate constant for dissociation of $NADP^+$ were measured spectrophotometrically using stopped-flow methods. A reaction mixture consisting of 20 μM *KMO* and 2 mM DTT, with or without saturating L-Kyn or inhibitor (*m*-NBA or BA), was prepared in a tonometer and made anaerobic by 45 alternating cycles of vacuum and argon gas at 5 °C. Saturating ligand concentrations were based on measured dissociation constants for each ligand for the oxidized enzyme complex (K_d = 17.4 μM for L-Kyn, K_d = 4.3 μM for *m*-NBA, and K_d = 7.6 μM for BA at 5 °C) (*22*). The tonometer was then mounted onto a Hitech DX2 stopped-flow spectrophotometer that had been scrubbed of residual oxygen for 12−15 h by the introduction of a solution of anaerobic glucose (50 mM) and glucose oxidase (62 units/mL). The enzyme complex was mixed against varied concentrations of anaerobic NADPH (100−3200 μM) prepared by 10 min of argon sparging. The reduction of the flavin was monitored by the decrease in the absorbance of the flavin at 450 nm. Each absorbance trace was fit to a sum of two exponentials according to eq 5.

$$A_{450nm} = \Delta A_1 e^{-k_1 t} + \Delta A_2 e^{-k_2 t} + C \quad (5)$$

From this equation, the absorbance amplitudes (ΔA) and associated rate constants were determined; C was the absorbance of the reduced flavin cofactor. The rate constant observed for the dominant phase was plotted against NADPH concentration and fit to a single-site binding equation according to eq 6, from which the constant for dissociation of NADPH from the KMO·ligand·NADPH complex (K_d) and the limiting rate of reduction (k_{RED}) were determined (*25*).

$$k_{obs} = k_{RED}[NADPH]/(K_d + [NADPH]) \quad (6)$$

Stopped-flow Measurements of the Oxidative Half-Reaction of KMO. The rate constants for observable steps of the oxidative half-reaction were measured spectrophotometrically using stopped-flow methods and unless stated otherwise were carried out without added NaCl. A reaction mixture typically consisted of ∼20 μM KMO, 3.5 μM xanthine oxidase, and 2 mM DTT with saturating L-Kyn or inhibitor (*m*-NBA or BA) was prepared in a tonometer and made anaerobic by 45 alternating cycles of vacuum and argon gas at 5 °C. Reduction was initiated by combining the reaction mixture with 400 μM xanthine and 5 μM methyl viologen from a sidearm, and reduction was allowed to proceed at 4 °C overnight (∼15 h). Saturating ligand concentrations were based on measured dissociation constants as determined by static titration of the oxidized enzyme and the reduction potentials measured in the presence of each ligand as detailed above and described below. The reduced anaerobic sample was then mounted onto a Hitech DX2 stopped-flow spectrophotometer that had been scrubbed of residual oxygen for 12−15 h by the introduction of an anaerobic solution of glucose and glucose oxidase. The enzyme complex was mixed with various concentrations of dioxygen (from ∼60 to 920 μM) prepared by sparging a solution of 20 mM HEPES buffer for 10 min with a defined ratio of nitrogen and oxygen gas delivered from a Maxtec maxblend gas blender and calibrated using an oxygen electrode. The absorbance and fluorescence changes that occurred in the oxidative half-reaction were monitored using both photomultiplier tube (PMT) and photodiode array (PDA) detection. In PMT mode, absorbance traces were collected at 415 nm, which was a convenient wavelength for observation of all three phases that occur in the half-reaction. Fluorescence was monitored by excitation at 380 nm and the observation of total emission. Each absorbance trace was fit to a sum of three exponentials, and the fluorescence traces were fit to a sum of two exponentials. Intermediate spectra were obtained by deconvolution of the PDA data sets using SpectFit (Spectrum Software Associates, Chapel Hill, NC) based on the rate constants measured in single-wavelength mode.

The effect of both NaCl and 3OHKyn on the kinetics of the oxidative half-reaction of *KMO* was also observed. An anaerobic sample of reduced *KMO* in complex with L-Kyn as detailed above was mixed with varied concentrations of NaCl (0−500 mM) or 3OHKyn (0−1.2 mM) in a solution of buffered 20 mM HEPES and 2 mM DTT (pH 7.5) equilibrated at 5 °C to yield a final dioxygen concentration of 920 μM after mixing. All absorbance traces were monitored at 415 nm and were analyzed using the methods described above.

H_2O_2 Quantification and Coupling to Hydroxylation. Evidence of the evolution of hydrogen peroxide from the KMO·*m*-NBA complex was obtained by dioxygen electrode assays in the presence and absence of catalase. KMO (10 μM) was mixed with limiting concentrations of NADPH (25−200 μM) and saturating inhibitory ligand under conditions of atmospheric oxygen (∼250 μM) in 20 mM HEPES (pH 7.5) at 25 °C with and without excess catalase (∼5 units/mL). The reaction was initiated by the addition of NADPH, and an initial rate was obtained for reaction times between 10 and 40 s. The rate of dioxygen consumption in the presence of catalase was then plotted versus the rate in the absence of catalase and fit to a straight line to determine the slope.

Evidence of the reaction stoichiometry with respect to hydroxylation for BA was obtained by product analysis using a Waters Delta 600 HPLC system. A standard curve for BA (0−500 μM) was prepared using an analytical (4.6 mm × 250 mm) Synergi phenyl reverse phase column. The maxima for BA absorption, 218 and 247 nm, were monitored using a Waters 2487 dual-wavelength absorbance detector coupled to a Waters 600 solvent delivery system. The flow rate was maintained at 1.00 mL/min, and the mobile phase was 50 mM phosphate buffer (pH 7.0). To test for the consumption of BA, reaction mixtures containing 10 μM KMO, varied concentrations of BA (100−200 μM), and limiting concentrations of NADPH (50−120 μM) were prepared. The reaction was stopped by filtering the mixture through a 0.5 mL Millipore 10 kDa molecular cutoff centrifugal filter

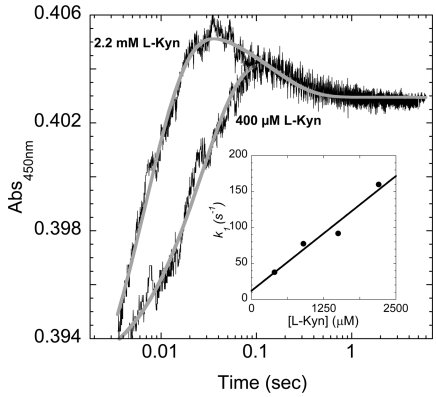

FIGURE 1: Substrate binding to oxidized KMO. The kinetics associated with the binding of native substrate, L-Kyn, to oxidized KMO were monitored on the stopped-flow spectrophotometer at 450 nm. A reaction mixture of 80 μM KMO and 4 mM DTT was mixed with pseudo-first-order concentrations of L-Kyn [400 μM to 2.2 mM (final concentration)] at 5 °C. The traces shown are for 400 μM and 2.2 mM L-Kyn. The inset depicts a linear fit to the measured values (●) of the rate constant for the first phase (k_1) for each of the L-Kyn concentrations that was used. The end of the flow is regarded as time zero.

device. The peak areas between the reaction mixture and control reaction (without KMO) were quantified and compared to define coupling with respect to hydroxylation.

RESULTS

L-Kyn Binding to Oxidized KMO. The binding of L-Kyn to oxidized KMO is relatively slow and causes perturbations of the flavin absorbance transitions (340−480 nm). The largest extinction coefficient change of ~400 M^{-1} cm^{-1} occurs at 450 nm (Figure 1). As such, there is a requirement that relatively high concentrations of enzyme (40 μM final concentration) be used to achieve an acceptable signal-to-noise ratio. This high enzyme concentration limits the L-Kyn concentrations that can be used to achieve pseudo-first-order reaction conditions (>400 μM). The data indicate that two phases were observed prior to equilibrium, suggesting that a reversible two-step binding model is sufficient to describe the association (eq 7) with the expression for the overall dissociation constant shown in eq 8

$$\mathrm{KMO_{OX}} + \text{L-Kyn} \underset{k_2}{\overset{k_1}{\rightleftharpoons}} \mathrm{KMO_{OX}}\cdot\text{L-Kyn*} \underset{k_4}{\overset{k_3}{\rightleftharpoons}} \mathrm{KMO_{OX}}\cdot\text{L-Kyn} \quad (7)$$

$$([\mathrm{KMO_{OX}}][\text{L-Kyn}])/([\mathrm{KMO_{OX}}\cdot\text{L-Kyn*}] + [\mathrm{KMO_{OX}}\cdot\text{L-Kyn}]) = (k_2/k_1)(k_4/k_3)/(1 + k_4/k_3) \quad (8)$$

The first phase had a clear L-Kyn concentration dependence, and plotting the observed rate constant versus ligand concentration gave a straight line with a non-zero intercept (Figure 1, inset). The forward rate constant (k_1) was calculated from the slope of this line and found to be (64 ± 1) × 10^4 M^{-1} s^{-1}, with a somewhat poorly defined *y*-intercept defining the dissociation rate constant (k_2) of 12.1 ± 10 s^{-1}. The second phase occurs with an apparent rate constant of 8.1 ± 1.1 s^{-1}. The value for this rate constant was largely unchanging with L-Kyn concentration. The overall K_d value for the KMO_{OX}·L-Kyn complex measured previously was 17.4 μM (*22*). However, since the fractional accumulation of KMO_{OX}·L-Kyn is not known due to the rate constants for the reversible steps being either poorly defined in the case of k_2 or not known in the case of k_4, only limits for the value of k_4 can be deduced. From eq 8, we can state that k_2 and k_4 must each be between 1 and 10 s^{-1}, and only values for which the product of the two rate constants is ~10 give the independently measured dissociation constant value.

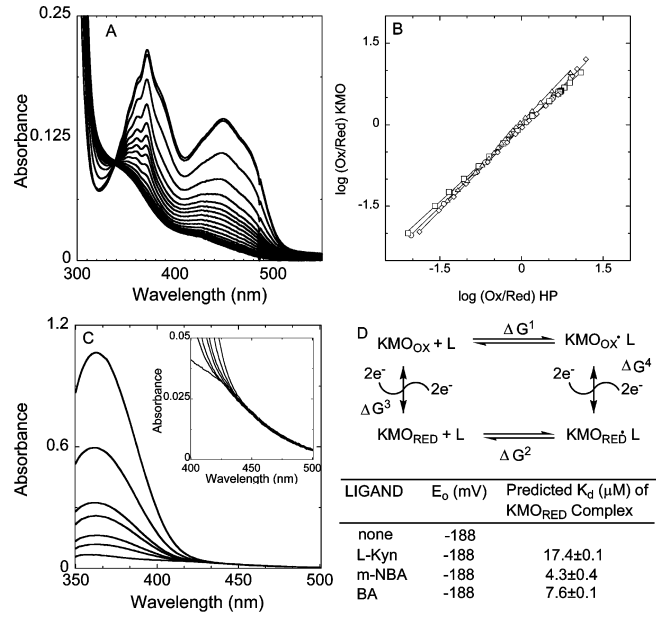

LIGAND	E_o (mV)	Predicted K_d (μM) of KMO_{RED} Complex
none	-188	
L-Kyn	-188	17.4±0.1
m-NBA	-188	4.3±0.4
BA	-188	7.6±0.1

FIGURE 2: Reduction potentials and substrate binding to the reduced enzyme. (A) Absorbance changes due to the reduction of unliganded KMO and 1-hydroxyphenazine (−187 mV), by xanthine oxidase. Enzyme and dye (10 μM each) were in the presence of 300 μM xanthine, 5 μM methyl viologen, and 500 nM xanthine oxidase. (B) Determination of the reduction potentials for KMO, KMO·L-Kyn, KMO·BA, and KMO·*m*-NBA complexes. The correlating value for KMO at the HP midpoint was used in the Nernst equation to calculate reduction potentials. (C) The spectra depict reduced *KMO* (10 μM) titrated L-Kyn (absorbance maximum at 363 nm) under anaerobic conditions at 5 °C. The inset is an expansion of the data at longer wavelengths. (D) A thermodynamic box linking ligand binding and flavin reduction events in KMO. The table lists the reduction potentials and predicted K_d values for the KMO_{RED}·L-Kyn, KMO_{RED}·*m*-NBA, and KMO_{RED}·BA complexes based on the measured reduction potentials.

Reduction Potentials and Ligand Affinities for the Reduced Enzyme. The reduction potentials of the free enzyme and ligand complexes were measured spectrophotometrically using a xanthine/xanthine oxidase reduction system (*24*). The dye used for these experiments was 1-hydroxyphenazine (HP; E'° = −187 mV). Initially, both HP and KMO_{free} were reduced separately by this system in measuring the extinction coefficients of the oxidized and reduced forms of both chromophores. Experiments in which the dye was mixed with KMO_{free}, KMO·L-Kyn, KMO·*m*-NBA, or KMO·BA were undertaken (Figure 2A). For KMO_{free} and for each KMO· ligand complex, the reduction potential was −188 ± 1 mV (Figure 2B,D), indicating that the binding of ligands did not modulate the reduction potential of the flavin.

An attempt was made to measure the binding isotherm for the reduced KMO·L-Kyn complex using spectral perturbation when the reduced free enzyme was titrated with L-Kyn under anaerobic conditions. The majority of the reduced flavin spectrum is obscured by the absorption spectrum of L-Kyn; however, the flavin spectrum at wavelengths greater than 440 nm is unobstructed. These data

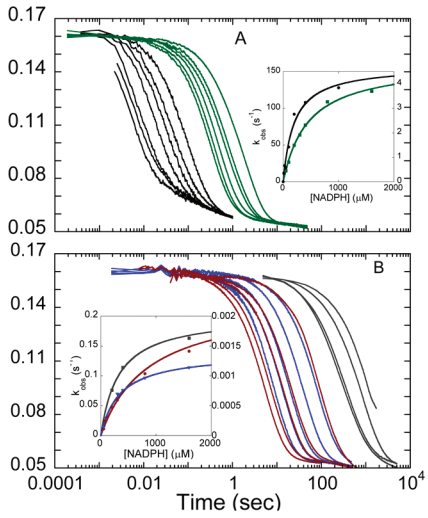

FIGURE 3: Dependence of the observed rate constant for reduction of KMO on the concentration of NADPH in the presence and absence of ligands. Anaerobic mixtures of 10 μM KMO and, where applicable, saturating ligand were mixed against anaerobic NADPH concentrations on a stopped-flow spectrophotometer at 5 °C. The decrease in flavin absorbance was observed at 450 nm. (A) Reduction traces of the KMO•L-Kyn complex in the absence (black lines) and presence (green lines) of 10 mM NaCl. The inset depicts the dependence of the observed reduction rate constant on the concentration of NADPH fit to eq 6 for the KMO•L-Kyn complex (black line, circles, left-hand *y*-axis) and the KMO•L-Kyn complex with NaCl (green line, squares, right-hand *y*-axis). (B) Reduction traces of the KMO•*m*-NBA complex (blue lines), the KMO•BA complex (red lines), and unliganded KMO (black lines) in the presence of 10 mM NaCl. The inset depicts the dependence of the observed reduction rate constant on the concentration of NADPH fit to eq 6 for KMO complexes: KMO•*m*-NBA (red line, circles, left-hand *y*-axis), KMO•BA (blue line, triangles, left-hand *y*-axis), and KMO (black line, squares, right-hand *y*-axis). All times shown are from the end of the flow.

indicated that no perturbation of the reduced flavin spectrum was discernible, preventing the direct measurement of the binding constant by these methods (Figure 2C). However, from E'° values and Hess's law, one can conclude that the K_d values of KMO_{OX}•L-Kyn (17.4 μM) (*22*) and KMO_{RED}•L-Kyn complexes are the same (Figure 2D). Similar correlations can be made for *m*-NBA and BA to define the concentration required to saturate the reduced enzyme prior to observing the oxidative half-reaction in the presence of these ligands.

Kinetics of the Reductive Half-Reaction. To observe reduction of the flavin cofactor by NADPH, oxidized KMO was mixed anaerobically with NADPH under pseudo-first-order conditions using a stopped-flow spectrophotometer. Reduction of the flavin was monitored at 450 nm, and the traces obtained were typically fit to a linear combination of two exponentials. The majority of flavin reduction was observed to be relatively rapid, and some small fraction occurred more slowly possibly due to sample heterogeneity. In all cases, the dependence of the observed rate constant of the dominant phase, in terms of amplitude change, on the concentration of NADPH was hyperbolic (Figure 3). In the presence of saturating L-Kyn and the absence of sodium chloride, the limiting rate constant for reduction was 158 ± 13 s^{-1} and a K_d for NADPH of 196 ± 44 μM was obtained (Figure 3A). The rate of reduction, therefore, does not limit the overall turnover number of the enzyme (~1.3 s^{-1}) (*22*). Acquisition and analysis of the data in the absence of NaCl were complicated by the turbidity accumulating in the enzyme solution; to avoid this complication, most subsequent reduction experiments were conducted in 10 mM NaCl which both slowed the reduction reaction and stabilized the enzyme. As such, reduction data acquired in the presence of this concentration of NaCl provide relative rather than absolute measures of reduction. In the experiments that included NaCl, >90% of the reduction occurred in a single phase (Figure 3A,B). The reduction of the KMO•L-Kyn complex occurred with a rate constant of 4.9 ± 0.3 s^{-1} and gave a K_d for the KMO•L-Kyn•NADPH complex of 377 ± 50 μM. This value for the limiting rate of reduction is 30-fold slower than that measured in the absence of NaCl, indicating that the reduction is strongly influenced by the added salt which has been observed for other FAH enzymes (*26, 27*). In the presence of 10 mM NaCl, the limiting rate constant for reduction of the KMO•L-Kyn•NADPH complex by NADPH was 2500-fold faster than the constant for reduction of the free enzyme that had an estimated limiting rate constant of ~0.0020 s^{-1}. Although flavin reduction in the absence of L-Kyn was slow, the dissociation constant for the KMO_{OX}•NADPH complex was 324 ± 31 μM, the same as that measured with saturating L-Kyn. As such, we can conclude that the binding of substrate does not diminish or enhance the ability of NADPH to bind the enzyme prior to reduction. Other structural factors must, therefore, contribute to the enhancement of the reduction rate constant. Collectively, these data indicated that the active site must be occupied by L-Kyn for rapid reduction by NADPH to occur.

KMO inhibitors also stimulated reduction of flavin by NADPH. BA stimulated the rate of reduction by 115-fold (0.229 ± 0.01 s^{-1}) and *m*-NBA by 70-fold (0.138 ± 0.006 s^{-1}) (Figure 3B). The NADPH dissociation constant observed for the KMO•*m*-NBA•NADPH complex was 346 ± 44 μM, similar to that observed for both the KMO•NADPH and KMO•L-Kyn•NADPH complexes. The constant for dissociation of NADPH from the KMO_{OX}•BA•NADPH complex was found to be 865 ± 97 μM, only 2.4-fold higher than that observed with the other effectors.

Additional KMO reduction experiments were conducted in the presence of a low concentration of NaCl (6 mM) (Figure 4). This concentration was chosen as a compromise to increase the rate of reduction and promote the accumulation of charge-transfer complexes while restraining the maximal rate constant so that reduction may be easily observed using stopped-flow methods. As in prior experiments, the data measured at 450 nm were predominantly monophasic and were fit to a limiting rate constant of 26.1 ± 0.1 s^{-1}. At longer wavelengths, a broad charge-transfer absorption band was observed, with an estimated maximal absorbance at ~700 nm. This absorbance accumulated relatively rapidly at 104 ± 1 s^{-1}, and its decay mirrored the observed rate constant for reduction. This charge-transfer absorbance band suggests proximity of the flavin isoalloxazine ring system to the nicotinamide ring in either the KMO_{OX}•L-Kyn•NADPH complex or the ensuing KMO_{RED}•L-Kyn•$NADP^+$ complex. The data can be fit to sequential steps of 104 s^{-1} followed by 26 s^{-1} or with the rate constants switched. In the former case, one would conclude that the charge transfer arises from the KMO_{OX}•L-Kyn•NADPH complex, while the latter would argue for the KMO_{RED}•L-Kyn•$NADP^+$ complex. It was possible to deduce that the

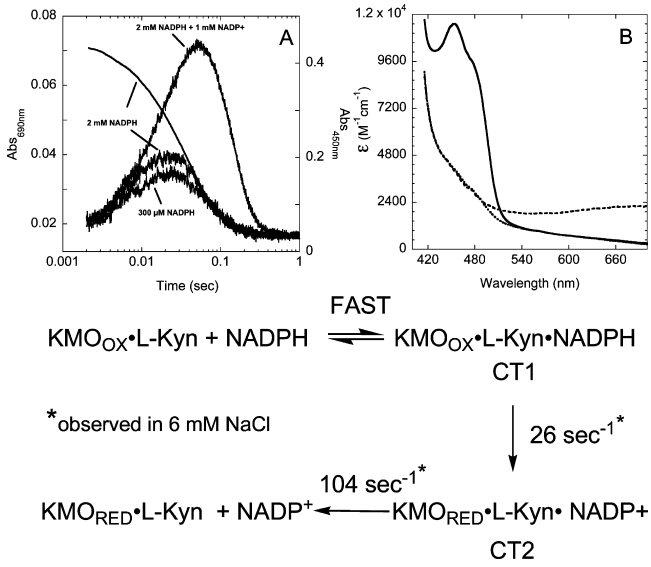

FIGURE 4: Reduction of the KMO_{OX}•L-Kyn complex by NADPH in the presence of 6 mM NaCl. The final anaerobic reaction mixture consisted of 50 μM KMO, 1 mM L-Kyn, and 4 mM NADPH in the presence of 1 mM DTT, 10 mM HEPES, and 6 mM NaCl (pH 7.5). (A) Data observed at 450 nm compared to that collected at 690 nm. (B) Deconvoluted absorbance spectra of the species observed during the reductive half-reaction for the reduction of KMO in the presence of saturating L-Kyn and NADPH when diode array data sets were fit to the kinetic model describing two successive first-order events. The end of the flow is regarded as time zero.

transition observed arose from the KMO_{RED}•L-Kyn•$NADP^+$ complex by comparing both the overall amplitude change at increasingly higher NADPH concentrations and the effect of exogenous NADP+ on the extent of accumulation of charge-transfer absorbance (Figure 4A). At higher NADPH concentrations, the rate of reduction increased hyperbolically until the enzyme was saturated in the reductant. One of the two rate constants observed for the charge transfer and decay mirrors the rate constant for reduction (maximum of $\sim$26 s^{-1}), while the other rate constant is ostensibly unchanging ($\sim$100 s^{-1}). The lack of dependence for this phase suggests that it is the decay of the KMO_{RED}•L-Kyn•$NADP^+$ complex that is observed and that the release of $NADP^+$ occurs with a rate constant of $\sim$100 s^{-1} (Figure 4A) (*28*). In addition, the inclusion of 1 mM $NADP^+$ dramatically enhances the accumulation of the charge-transfer absorbance via exchange with the KMO_{RED}•L-Kyn•$NADP^+$ complex, prolonging its decay. If the alternate KMO_{OX}•L-Kyn•NADPH complex were observed, we would expect exogenous $NADP^+$ to decrease the extent of charge-transfer accumulation by competition for the active site slowing of the reduction of the flavin. The deconvoluted intermediate spectrum of the charge-transfer complex based on this model is depicted in Figure 4B. These spectra are consistent with the assertion that only KMO_{RED}•L-Kyn•$NADP^+$ complex charge transfer is observed as the intermediate spectrum has characteristics of both the reduced enzyme and a broad charge-transfer absorption band ($\varepsilon_{700} \sim 1000$ M^{-1} cm^{-1}) (*29*−*31*).

Kinetics of the Oxidative Half-Reaction. The latter half of the catalytic cycle occurs when $NADP^+$ has dissociated and the reduced enzyme substrate complex reacts with dioxygen. To observe intermediates that arise during the oxidative half-reaction, the anaerobic reduced KMO•L-Kyn complex was mixed with pseudo-first-order dioxygen concentrations using a stopped-flow spectrophotometer. Additional insight into the oxidative mechanism was obtained by the use of the two substratelike inhibitors *m*-NBA and BA that have deactivated and nonactivated aromatic rings, respectively, relative to L-Kyn.

Triphasic absorbance traces were observed for the KMO_{RED}•L-Kyn complex in reaction with dioxygen, suggesting two spectrally distinct intermediates form during the hydroxylation and reoxidation reactions. The observed rate constant of the first phase exhibited a linear dependence on molecular oxygen concentration with a zero intercept indicating a second-order reaction with a rate constant of (1.5 ± 0.1) $\times$ 10^5 M^{-1} s^{-1} (Figure 5A, inset). The two subsequent phases were not oxygen-dependent and had measured rate constants of 5.5 ± 0.9 and 1.9 ± 0.6 s^{-1} (Figure 5A). The first phase was attributed to the collision of the reduced flavin with dioxygen that forms a one-electron-oxidized flavin and superoxide pair that rapidly collapse to form a C4a-peroxyflavin that is immediately protonated to give an electrophilic hydroperoxyflavin species. This is based on the requirement for triplet ground-state dioxygen to be reduced via single electron steps to facilitate a necessary electron spin inversion event and for the flavin−peroxy species to be protonated to have electrophilic character. In the deconvoluted intermediate spectra, the first species that accumulates after mixing with dioxygen is characteristic of a flavin C4a-oxygen adduct and includes no evidence of a contribution from the product 3OHKyn that has a maximum absorption at 380 nm. The second phase is assigned as the hydroxylation event and results in the accumulation of absorption bands consistent with the oxidized enzyme. This indicates that the C4a-hydroxyflavin expected to arise concomitant with hydroxylation of L-Kyn decays rapidly and does not have significant accumulation in the half-reaction (Figure 5B). In addition, fluorescence emission traces confirm that no evidence of the normally highly fluorescent hydroxyflavin species is observed; instead, these data show only a modest increase in fluorescence due to the re-formation of the oxidized flavin (Figure 5A). It is inferred therefore that the hydroxyflavin is prone to rapid dehydration immediately after the hydroxylation of L-Kyn.

The final and rate-limiting phase of the KMO•L-Kyn oxidative half-reaction involves a change in the shape of the oxidized enzyme spectrum and suggests that a conformational change(s) attends the final phase. Given that the second to last and final species both have a spectrum of the oxidized enzyme, they must arise after hydroxylation of L-Kyn. It is therefore conceivable that the final phase is associated with the release of the product, 3OHKyn. To test the involvement of the product in the final step, various concentrations of 3OHKyn in the presence of pseudo-first-order dioxygen were mixed with the KMO_{RED}•L-Kyn complex on the stopped-flow instrument. These data indicated that the rate constant measured for the last phase remained constant while the amplitude associated with this step decreased as a function of increasing 3OHKyn concentration (Figure 6A). The amplitude change for this step had a hyperbolic dependence on 3OHKyn concentration, which is presumably a result of the repopulation of the active site of the enzyme by exogenous 3OHKyn after the nascent 3OHKyn is released, effectively locking the enzyme in the second intermediate form. In addition, the difference spectra of the penultimate

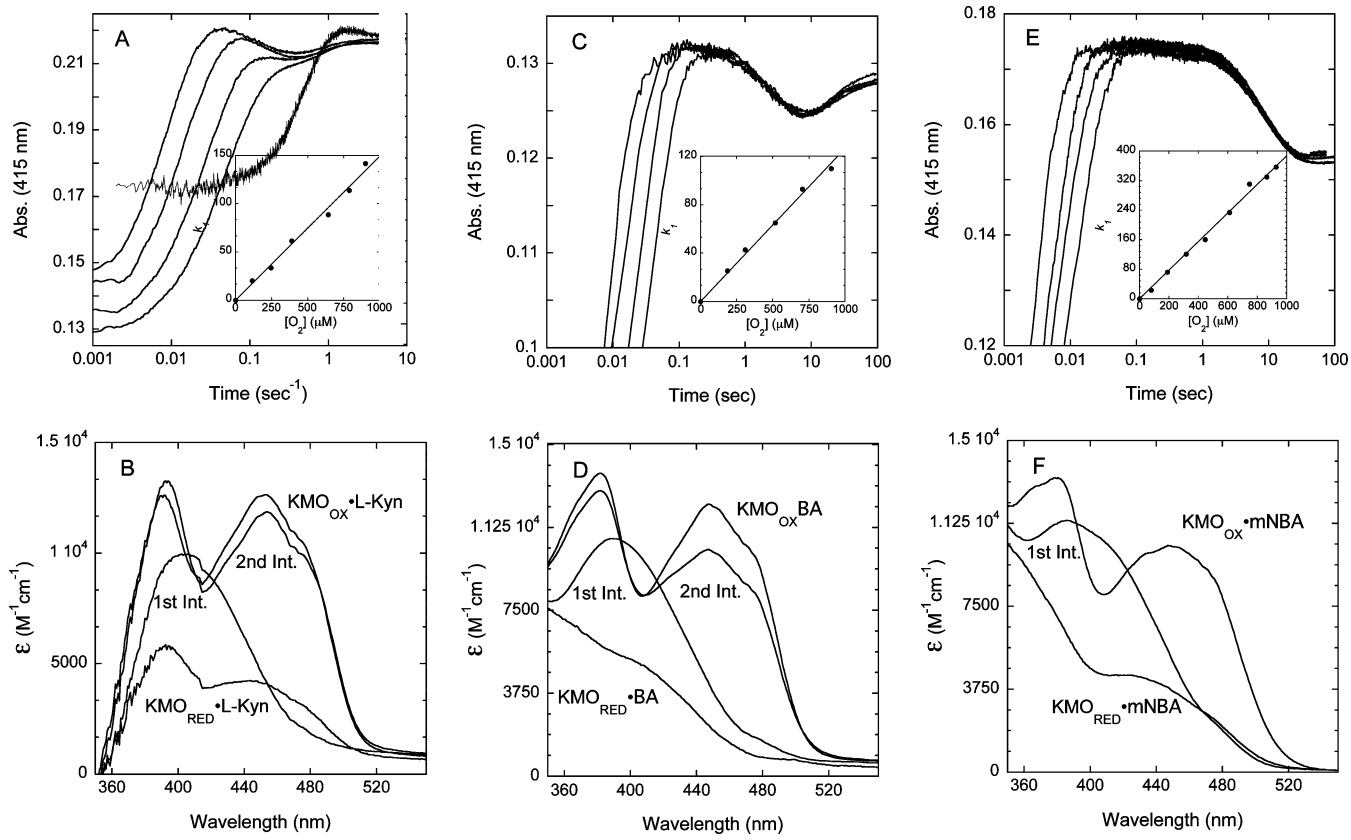

FIGURE 5: Oxidative half-reaction of KMO in the presence of saturating L-Kyn, BA, and *m*-NBA. Anaerobic mixtures of 18.5−16.5 μM KMO_{RED}, 1 mM DTT, and saturating ligand (L-Kyn, *m*-NBA, and BA) were mixed against pseudo-first-order dioxygen concentrations using a stopped-flow spectrophotometer at 5 °C. The changes in intermediate absorbances were observed at 415 nm. (A) Absorbance traces for KMO_{RED}•L-Kyn complex reoxidation at various dioxygen concentrations. A single emission trace depicts the fluorescence changes observed when the compound is excited at 380 nm. The inset depicts the dependence of the observed value for the rate constant, k_1, on the concentration of dioxygen fit to a straight line. (B) Deconvoluted pure absorption spectra of the species observed during the oxidative half-reaction in the presence of saturating L-Kyn. To obtain the pure intermediate spectra, the unbound L-Kyn absorbance contrubution (381 μM) was subtracted from all spectra. The final two spectra were adjusted by subtraction of the 3OHKyn contribution from the absorption spectrum (18.5 μM). (C) Reoxidation of the KMO_{RED}•BA complex observed at 415 nm. The inset depicts the dependence of the observed value for the rate constant, k_1, on the concentration of dioxygen fit to a straight line. (D) Pure deconvoluted intermediate spectra observed in the reoxidation of the KMO_{RED}•BA complex. (E) Reoxidation of the KMO•*m*-NBA complex as observed at 415 nm. The inset depicts the dependence of the observed value for the rate constant, k_1, on the concentration of dioxygen fit to a straight line. (F) Pure deconvoluted intermediate spectra observed in the reoxidation of the KMO_{RED}•*m*-NBA complex. The end of the flow is regarded as time zero.

and final species exhibit spectral perturbation similar to those associated with 3OHKyn binding to the oxidized enzyme (though inverted due to the conventional order of subtraction) (Figure 6A, inset). The overarching conclusions are that the final step in catalysis is 3OHKyn release and that this involves a conformational shift to a position that is the resting state of the unliganded oxidized enzyme. Further experiments conducted with *m*-NBA and BA indicate that the resulting difference spectra for the binding of each ligand (Figure 6B) were qualitatively the inverse of that observed for the binding of 3OHKyn, suggesting that these ligands promote a flavin environment change that is similar to what occurs during product release.

Despite the fact that hydroxylation is not occurring (see below), reoxidation of KMO in the presence of saturating BA revealed data similar to those obtained with L-Kyn (Figure 5C,D). The first phase was linearly dependent upon the dioxygen concentration and was followed by two events that were independent of dioxygen concentration. The rate constants measured were $(12 \pm 0.2) \times 10^4$ M^{-1} s^{-1}, 0.39 ± 0.10 s^{-1}, and 0.044 ± 0.007 s^{-1}. Multiwavelength diode array data were deconvoluted to reveal a single flavin adduct intermediate that forms in the first phase that then decays to yield the spectrum of the oxidized enzyme. Interestingly, the enzyme then appears to undergo a product release-like step involving perturbations of the flavin spectrum similar to those observed after hydroxylation of the native substrate despite the fact that hydroxylation has not occurred. This suggests that the formation of the hydroperoxyflavin forces the enzyme into a conformation that can be relieved only by a conformational shift that is somewhat independent of the ligand that occupies the active site of the enzyme. This is analogous to what was observed in the study of the oxidative half-reaction of anthranilate hydroxylase in the presence of low concentrations of salicylate, where the hydroperoxyflavin was observed to accumulate and an additional event was observed after full reoxidation of the enzyme despite the fact the salicylate was not hydroxylated (*32*).

Similar oxygen-dependent kinetic experiments were conducted with KMO_{RED} in complex with *m*-NBA. For this ligand, the absorbance traces observed at 415 nm were biphasic with a long-lived first intermediate that decayed with a half-life of 5 s. The rate constant for formation of this intermediate was again linearly dependent upon oxygen, and the line of best fit passed through the origin, indicating a collision-based process (Figure 5E, inset) with a rate constant

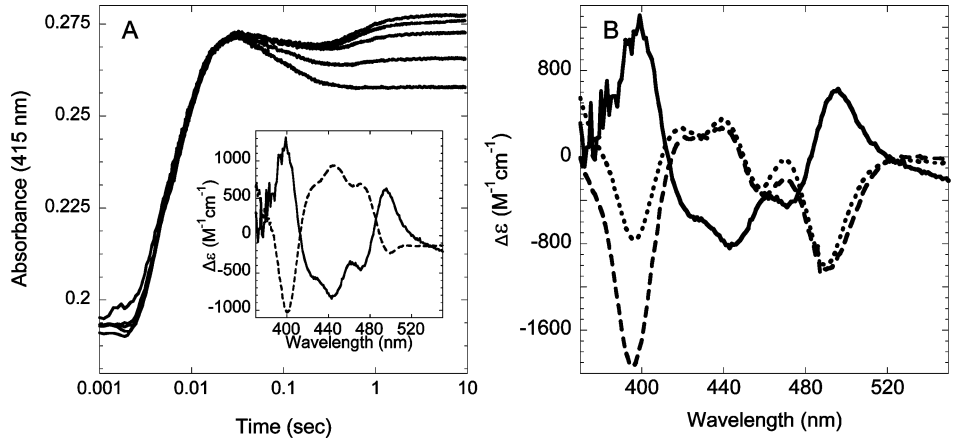

FIGURE 6: Spectrophotometric evidence of two recurring flavin environments. (A) The suppression of the amplitude of the third phase in the oxidative half-reaction in the presence of saturating L-Kyn and 924 μM dioxygen by increasing the exogenous concentration of the product 3OHKyn (0−1.2 mM). The inset illustrates the difference spectra of the product release step (---) and that of 3OHKyn binding. All times are from the end of the flow. (B) The absorption changes of the KMO_{OX} flavin spectrum upon binding of saturating 3OHKyn (—), *m*-NBA (•••), and BA (---).

of (38.7 ± 0.5) × 10^4 M^{-1} s^{-1}. The spectrum of the intermediate observed was again suggestive of a flavin−oxygen adduct that can be surmised to be the flavin−hydroperoxide species due to the stoichiometric liberation of hydrogen peroxide observed in the presence of this ligand (see below). The second phase did not exhibit an oxygen dependence, occurred with a relatively slow rate constant of 0.10 ± 0.01 s^{-1}, and coincided with the decay of a C4a-hydroperoxyflavin intermediate to yield the oxidized enzyme. Unlike the data obtained with L-Kyn and BA, a third kinetic phase suggestive of a product release-like step was not observed. In addition, the final absorbance spectrum of the reoxidized flavin at 450 nm was 10300 M^{-1} cm^{-1}, around 2000 M^{-1} cm^{-1} lower than that of the free oxidized enzyme (12300 M^{-1} cm^{-1}), suggesting that the ligand has not dissociated from the enzyme after decay of the hydroperoxyflavin and that the flavin is locked in an environment that is dissimilar from that of either the product complex or free enzyme. However, as KMO consumes superstoichiometric amounts of dioxygen in the presence of *m*-NBA, it is conceivable that the final *m*-NBA complex is competent in reduction and that *m*-NBA has no requirement for dissociation between oxidative and reductive phases of catalysis. This is one possible explanation for the relatively high inhibitory capacity of this ligand with KMO as evidenced by the low IC_{50} values observed for this inhibitor with the mammalian form of the enzyme (~900 nM), which differ significantly from the K_d value measured in titration of *m*-NBA to the oxidized bacterial enzyme (8 μM) (*22, 33*) (Scheme 2).

Effect of Anions on the Oxidative Half-Reaction. The rate constants measured for individual steps of the oxidative half-reaction are sensitive to the presence of NaCl. It can reasonably be concluded that the effect is solely from the added chloride ions as no inhibitory effect from sodium has been observed when buffer solutions are titrated with NaOH and the enzyme is not sensitive to ionic strength in the low to mid-millimolar range. Moreover, the influence of anions on the catalysis of class A FAHs is well-documented (*28, 34−36*). To observe this effect on the oxidative half-reaction, the anaerobic reduced KMO•L-Kyn complex was mixed with varied NaCl concentrations and pseudo-first-order dioxygen (~920 μM) using a stopped-flow spectrophotometer. The observed absorbance traces were fit to a linear combination of three exponentials. As the NaCl concentration was increased, the amplitude associated with the third phase decreased and by 5 mM NaCl had been almost entirely suppressed (Figure 7A). As proposed above, the third phase is the product release step, and therefore, the saturation of the oxidized enzyme with Cl^- either inhibits product release or forces the flavin into an environment that mimics the product-bound state. The dissociation constant based on the plot of the amplitude change versus chloride ion concentration indicates a relatively high affinity of 0.77 ± 0.23 mM (Figure 7A, inset). Further titration of NaCl to a concentration of 100 mM slows the rate constant associated with the second phase of the half-reaction assigned here as decay of the rate constant for hydroxylation. The rate constant is observed to decrease to a plateau (Figure 7B), and the constant for dissociation of chloride ions from the hydroperoxyflavin was determined to be 3.5 ± 0.8 mM (Figure 7B, inset). These data are consistent with kinetic and structural evidence of anion association in other FAH enzymes (*35, 37*) but do not distinguish between single or multiple anion binding sites.

Stoichiometry of Formation of H_2O_2 from KMO Inhibitor Complexes. Enzymes in the FAH family are uniformly believed to stabilize the weak hydroperoxyflavin electrophile that is capable of hydroxylating only activated aromatic rings. The two inhibitors, *m*-NBA and BA, have relatively unactivated rings, and when reduction of the enzyme was stimulated by the presence of these inhibitors, it was surmised that this would lead to NADPH oxidase activity and the production of H_2O_2 in place of hydroxylation of the aromatic ring. For *m*-NBA, formation of hydrogen peroxide was quantified by monitoring the rate of dioxygen consumption in the presence and absence of an excess of catalase with respect to KMO activity (Figure 8A). The reaction including catalase consistently exhibited half the rate of dioxygen consumption relative to the reaction without catalase, confirming that one molecule of H_2O_2 is liberated with each molecule of NADPH consumed in the presence of these inhibitors (Figure 8B).

For BA, the data obtained by these methods were less consistent and seemed to suggest some degree of coupling of reduction to hydroxylation. Product analysis using HPLC, however, indicated that the KMO_{RED}•BA complex is, within

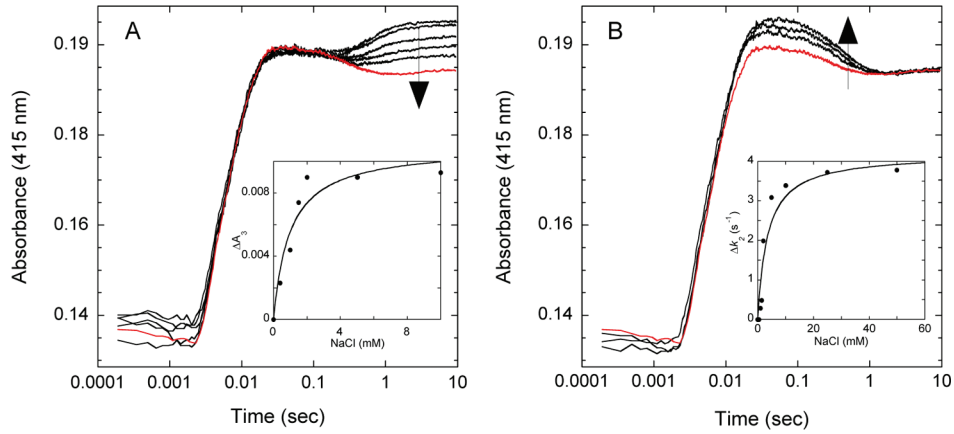

FIGURE 7: Influence of chloride ions on the oxidative half-reaction of the KMO_{RED}•L-Kyn complex. (A) Decrease in the amplitude of the third phase observed with an increase in NaCl concentration from 0 to 5 mM. Traces shown are for 0, 0.4, 1, 1.5, 2.0, and 5.0 mM NaCl. The inset depicts the change in amplitude of the third phase plotted vs NaCl concentration and fit to a single-site binding equation. (B) Decrease in the rate constant of the second phase when the NaCl concentration is increased from 5 to 50 mM. The inset depicts the change in the rate constant of the second phase relative to the rate constant observed in the absence of NaCl plotted vs NaCl concentration and fit to a single-site binding equation. The trace observed at 10 mM NaCl is common to both panels A and B and is colored red. The end of the flow is regarded as time zero.

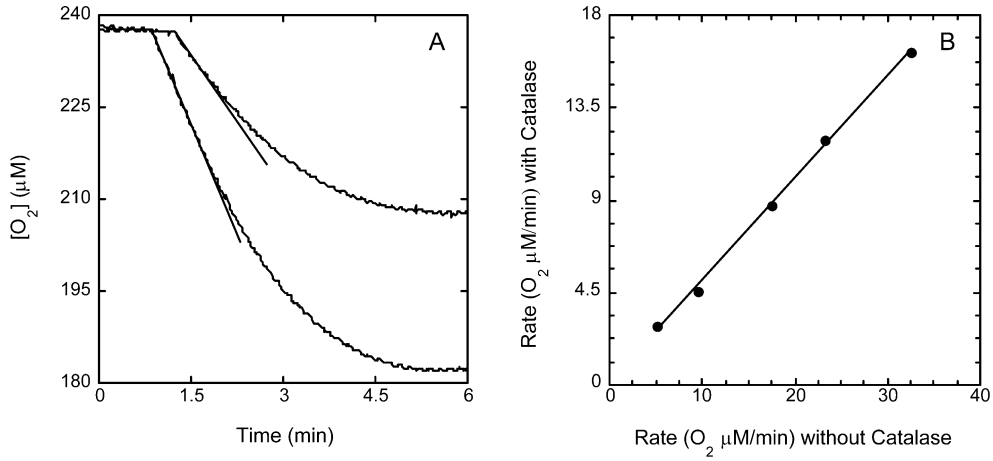

FIGURE 8: Stoichiometry of the evolution of H_2O_2 from the KMO_{RED}•*m*-NBA complex. Each oxygen probe assay contained a mixture that consisted of saturating ligand (300 μM *m*-NBA and 600 μM BA), 10 μM KMO, and varied concentrations of NADPH (50−250 μM). Each assay was performed in the presence and absence of excess catalase activity. (A) Two representative oxygen probe assays with and without catalase (highest rate). Straight lines are tangents to the early time frames and were used to define the initial rate of oxygen consumption. (B) Rate observed in the absence of catalase plotted vs the rate observed in the presence of catalase fit to a straight line with a slope of 0.5.

the limits of error, uncoupled. With a limiting level of NADPH, 92 ± 7% of the added BA was recovered in the filtrate from the KMO reactions, the discrepancy being ascribed to the fraction of BA that remains bound to the enzyme in the filtrand. The reasonable conclusion is that, like the *m*-NBA-stimulated KMO reaction, this complex is stoichiometrically producing H_2O_2 in place of hydroxylation.

DISCUSSION

Stroke is one of the leading causes of death, particularly in western societies. Each year in the United States, ~780000 people experience a stroke. Ischemic stroke is caused by occlusion of an artery to the brain and is the most common form of stroke (*38*). A lack of oxygen in the brain causes an abnormally high release of glutamate that causes excessive stimulation of neurons via its action at NMDA receptors. This results in cell death via a non-self-limiting cascade of glutamate release that ultimately results in brain eodema, diminished interstitial space, destruction of the blood−brain barrier, and lasting impairment or death (*3, 6*). Molecules that block glutamate interaction at NMDA receptors are touted as promising approaches for treatment of ischemic events (*2, 39, 40*). NMDA receptor antagonists and agonists are synthesized from tryptophan catabolism, and one in particular, kyurenate, has the ability to suppress glutamate release. It is thus desirable to alter the normal flux of metabolites through this pathway to weaken the agonists and/or enhance the antagonists. The available data suggest that the targeted inhibition of KMO is a viable strategy for achieving local elevation of kynurenate concentrations and limit the effects of heightened glutamate during oxygen debt (*3, 41−43*).

The central position of KMO in tryptophan catabolism with regard to metabolite accumulation is well-known (Scheme 3) (*44*), as is the need to develop molecules that modulate the activity of KMO for therapeutic purposes (*5*). However, mammalian forms of this enzyme are expressed at low levels constitutively, are not overexpressed in

Scheme 4

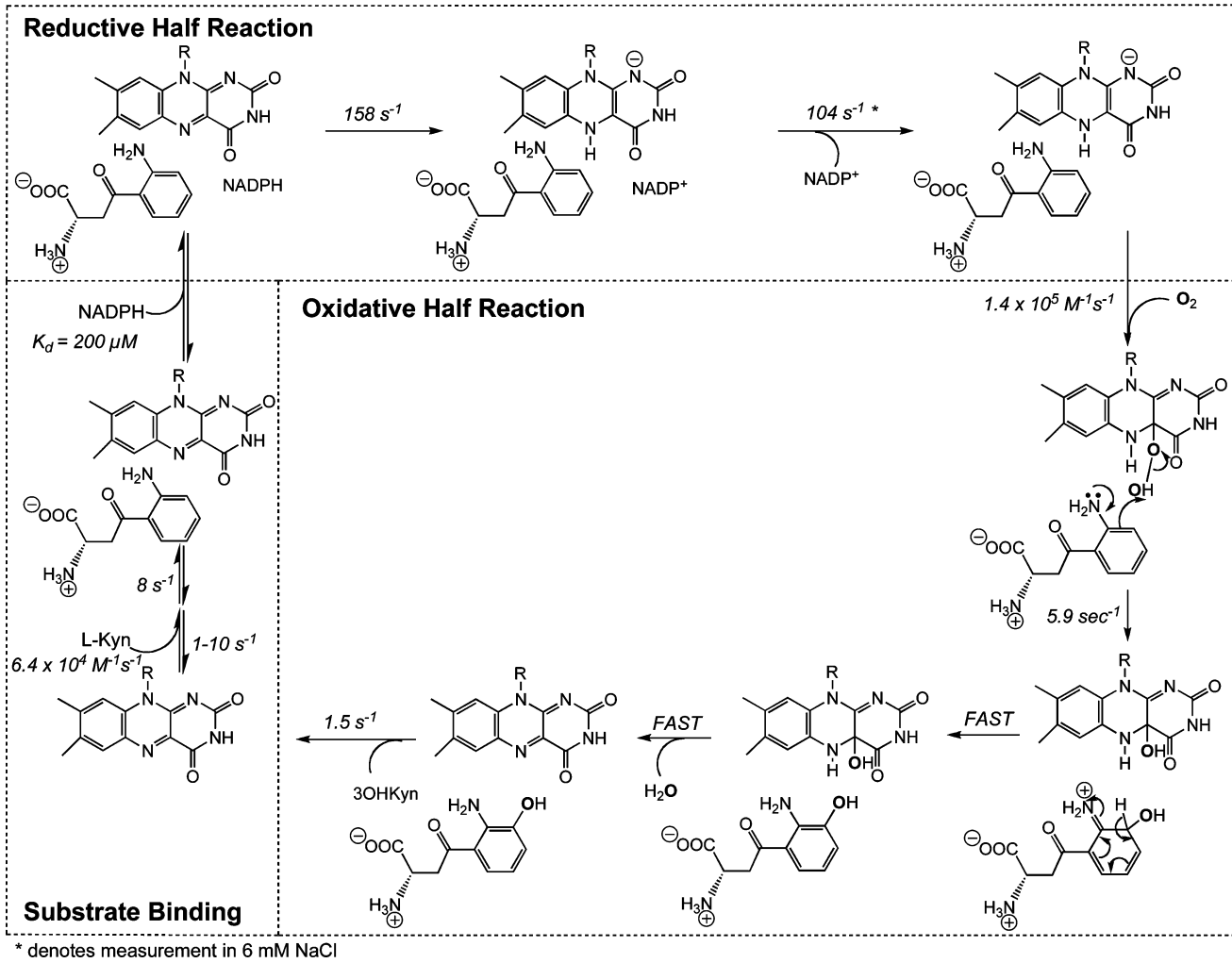

* denotes measurement in 6 mM NaCl

significant quantity heterologously, and have been shown to exhibit marked instability during isolation (*19, 20*). KMO from *P. fluorescens* is the only form of KMO known to be amenable to biophysical investigation and is therefore the prototypical form from which mechanism as it relates to inhibition can be investigated (*22*). In this study, we measured the rate constants and/or equilibrium constants associated with each of the observable steps that contribute to the overall turnover number of KMO. These values are summarized with the proposed chemical mechanism shown in Scheme 4. From these data, the predicted limiting rate of turnover of KMO is 1.16 s^{-1} [calculated using Chemical Kinetics Simulator (IBM)], in good agreement with the measured overall turnover number determined from steady-state analysis of 1.27 s^{-1} (*22*), and indicates that the enzyme as purified is fully active. Our data show that product release is the primary rate-limiting step in catalysis and that the stimulation of reduction of the flavin by NADPH is not contingent on recognition of an activating aromatic ring substituent as is the case for the paradigm FAH enzymes (*14, 15, 46, 47*). Moreover, the stabilization of a flavin−C4a-hydroperoxyflavin in the presence of a nonactivated substratelike inhibitor suggests that the events of the oxidative half-reaction are also less reliant on the interaction of the activating ring substituent with the enzyme which has been observed for other FAH enzymes that hydroxylate phenols. The inevitable liberation of the reduced dioxygen as hydrogen peroxide by the enzyme in the presence of these inhibitors strongly suggests that different routes to inhibition of KMO should be pursued if viable strategies for the treatment of brain ischemia are to be achieved from suppression of KMO activity.

Detailed analysis of the reaction mechanism of KMO has not previously been conducted. Our studies have shown that KMO is a member of the class A flavoprotein hydroxylases in that the reduction of the flavin by NADPH is stimulated 10^3-fold by the binding of L-Kyn, and in the absence of this substrate, flavin reduction occurs over long time intervals (~5000 s) (*10*). There is thus a mechanism for alerting KMO to the presence of the aromatic substrate to couple L-Kyn binding to hydroxylation which has been observed for other FAH enzymes (*14, 46, 48*). Unexpectedly, KMO inhibitors that mimic the substrate structure, such as *m*-NBA and BA, also stimulate reduction of the flavin by NADPH by 10^2-fold and therefore must be recognized as effectors for catalysis. Since neither *m*-NBA nor BA has a substituent that mimics the amino group of the native substrate's aniline ring, it can be concluded that, unlike the paradigm FAH enzymes whose activity is contingent on detection of the phenol ring hydroxyl group, the amine of L-Kyn does not appear to play a critical role in KMO sensing the presence of the substrate and it is the presence of some other group, such as the benzoyl carbonyl, that is required for substrate recognition. However, the 2-amino group of the L-Kyn

aniline ring is required for maximal rates of reduction to occur, suggesting that this group does serve to optimize the reaction to some degree.

It is accepted that the nicotinamide and isoalloxazine rings must be oriented in the proximity of each other to facilitate hydride transfer during reduction. Evidence would suggest that FAH enzymes require what has been described as a flavin "out" conformation for these two ring structures to contact each other. This is where the isoalloxazine exits the relatively confined and buried active site by pivoting at the 2-carbon of the ribosyl to make contact with the nicotinamide ring at the protein surface (*36, 49, 50*). The sequence of steps by which each FAH enzyme accomplishes this seems to vary. PHBH and PHHY both possess mechanisms that sense the presence of substrate phenol hydroxyl, which prompts flavin to move out with the binding of NADPH (*14, 36*). *m*-Hydroxybenzoate hydroxylase (MHBH), in contrast, has been shown crystallographically to reside in a flavin out conformation with the aromatic substrate bound (*48*). The final step of the reductive half-reaction is the egress of $NADP^+$ and the movement of the isoalloxazine ring to the in position. It has been posited that the negative charge of the reduced flavin cofactor induces withdrawal of the isoalloxazine to the relative positive electrostatic environment of the active site (*51*). At this point, the reduced enzyme−substrate complex is poised to react with dioxygen.

No definitive evidence of multiple flavin positions in the reductive half-reaction of KMO can be gleaned from the experiments presented here. However, a broad charge-transfer absorbance band is observed for the KMO_{RED}·L-Kyn·$NADP^+$ complex, allowing the $NADP^+$ dissociation rate constant (104 s^{-1}) to be measured. This differs from what is observed with PHBH where charge-transfer absorption bands for both the E_{OX}·S·NADPH and E_{RED}·S·$NADP^+$ complexes are observed (*29, 51*−*53*).

For the FAH enzymes, it is thought that the oxidative half-reaction begins with a one-electron reduction of dioxygen by the reduced flavin (*54*). The radical pair formed then rapidly collapses to yield a C4a-peroxyflavin that is then immediately protonated. Once formed, the hydroperoxyflavin then undergoes an electrophilic substitution reaction with the aromatic ring of the substrate, and the distal oxygen is delivered to one of the activated ring positions (typically ortho). This yields a C4(a)-hydroxyflavin and the product which is the second intermediate typically observed in single turnover with the native substrate. The decay of this species is thought to happen in a manner concomitant with product release and is often the rate-determining step of turnover (*16*). The oxidative half-reaction of KMO is comparable to what is described above; however, some differences arise due to both the balance of rate constants for successive steps and the sequence of events that follow hydroxylation. Unlike other FAH enzymes, the C4(a)-hydroxyflavin intermediate is not observed to accumulate in the KMO reaction. Instead, the second intermediate has a spectrum indicative of the oxidized enzyme. The conclusion is that for KMO, dehydration of the hydroxyflavin is not contingent on the release of the product and occurs rapidly. The difference spectrum of the second intermediate and the final species strongly suggests that the second intermediate is the KMO_{OX}· 3OHKyn complex. Product release then follows, observed as a small increase in the intensity of the flavin absorption transitions that are the reciprocal of those that occur when 3OHKyn is bound to the oxidized enzyme (Figure 6A, inset).

The reoxidation of the enzyme in the presence of BA or *m*-NBA gives absorbance data similar to those observed with L-Kyn. When mixed with dioxygen in the presence of either ligand, the enzyme initially accumulates an intermediate whose spectrum is consistent with and can be surmised to be that of the hydroperoxyflavin. With either ligand, this species then decays, liberating hydrogen peroxide and the oxidized enzyme without hydroxylation of the aromatic ring. For BA, however, an additional phase is then observed that involves a change in the shape of the oxidized enzyme spectrum. The difference spectrum of this second intermediate and the final species, while unique to this reaction, is similar to that observed for the product release step in the presence of the native substrate. For phenol hydroxylating enzymes, deactivated or unactivated substrates also result in the liberation of H_2O_2 during enzyme reoxidation (*30*). It is, however, rare for these enzymes to stabilize the hydroperoxyflavin in the presence of ring-deactivated ligands. The extended half-life of the hydroperoxyflavin in this case and more particularly in the presence of *m*-NBA says that the oxidative half-reaction is not immediately abortive in the presence of the wrong ligand, further supporting the idea that KMO does not rely on the detection of distinguishing substrate ring substituents at key points in catalysis. KMO instead advances through the steps of reduction, peroxyflavin formation, and decay, and then a product release-like step despite the fact that the substrate was not bound and the product was not formed. These data indicate that the product release step is built into the catalytic mechanism once the C4a-hydroperoxyflavin has formed.

One of the more allusive and curious aspects of the FAH catalytic mechanism is the proposed dynamic motion of the isoalloxazine during catalysis that is thought to control the binding and release of ligands to and from the active site (coined as the "wavin' flavin"). This phenomenon has been studied in great detail for PHBH and to a lesser extent for PHHY and MHBH, all of which have structures that confirm multiple discrete positions for the ring system (*35, 46, 48*). For KMO, no direct evidence in support of the flavin "wave" is offered here. However, evidence suggests two distinct flavin states are involved in the product release step. The similarity of the difference spectra for the binding of *m*-NBA and BA with that of the product release step (k_3) and in the mirror image of these spectral changes observed with the binding of 3OHKyn is clear evidence that the flavin encounters a small number of specific and recurring influences in response to ligand binding (Figure 6).

Low concentrations of anions induce changes in the KMO flavin spectrum similar to those observed with 3OHKyn. Like PHBH, KMO is sensitive to inhibition by anions and appears to bind one or more ions in the proximity of the active site, and occupancy of the anion site(s) has a direct influence on the flavin (*35*). This is observed with the suppression of the amplitude associated with the product release step to the point where the final spectrum resembles the spectrum of the product-bound form of the enzyme. It is thus a possibility that KMO is behaving like PHBH, where the balance of occupancy of known flavin positions is sensitive to local electrostatic changes.

CONCLUDING REMARKS

Despite the low level of sequence identity with other FAH enzymes, the reductive and oxidative half-reactions of KMO show marked similarity to that observed for the paradigm class A enzymes. The clear similarities are the stimulation of reduction by NADPH with aromatic substrate binding, the sensitivity to anions in both half-reactions, and flavin conformational changes during product release. The primary difference is that KMO appears to be less capable of discerning between the native substrate and substratelike molecules leading directly to NADPH oxidase activity and the liberation of hydrogen peroxide that in the case of BA and *m*-NBA would exacerbate attempts to use these molecules therapeutically. These data underscore the value of detailed in vitro enzyme−inhibitor interaction studies, such that an inhibitor's structure can be developed using both evidence of binding from IC_{50} or K_d values and mechanistic information.

REFERENCES

1. Botting (1995) Chemistry and Neurochemistry of the Kynurenine Pathway of Tryptophan Metabolism. *Chem. Soc. Rev. 24*, 401–412.
2. Carpenedo, R., Chiarugi, A., Russi, P., Lombardi, G., Carla, V., Pellicciari, R., Mattoli, L., and Moroni, F. (1994) Inhibitors of kynurenine hydroxylase and kynureninase increase cerebral formation of kynurenate and have sedative and anticonvulsant activities. *Neuroscience 61*, 237–243.
3. Moroni, F., Carpenedo, R., Cozzi, A., Meli, E., Chiarugi, A., and Pellegrini-Giampietro, D. E. (2003) Studies on the neuroprotective action of kynurenine mono-oxygenase inhibitors in post-ischemic brain damage. *Adv. Exp. Med. Biol. 527*, 127–136.
4. Giorgini, F., Guidetti, P., Nguyen, Q., Bennett, S. C., and Muchowski, P. J. (2005) A genomic screen in yeast implicates kynurenine 3-monooxygenase as a therapeutic target for Huntington disease. *Nat. Genet. 37*, 526–531.
5. Robotka, H., Toldi, J., and Laszlo, V. (2008) L-Kynurenine: Metabolism and Mechanism of Neuroprotection. *Future Neurol. 3*, 169–188.
6. Carpenedo, R., Pittaluga, A., Cozzi, A., Attucci, S., Galli, A., Raiteri, M., and Moroni, F. (2001) Presynaptic kynurenate-sensitive receptors inhibit glutamate release. *Eur. J. Neurosci. 13*, 2141–2147.
7. Pellicciari, R., Natalini, B., Costantino, G., Mahmoud, M. R., Mattoli, L., Sadeghpour, B. M., Moroni, F., Chiarugi, A., and Carpenedo, R. (1994) Modulation of the kynurenine pathway in search for new neuroprotective agents. Synthesis and preliminary evaluation of (m-nitrobenzoyl)alanine, a potent inhibitor of kynurenine-3-hydroxylase. *J. Med. Chem. 37*, 647–655.
8. Stone, T. W. (2000) Development and therapeutic potential of kynurenic acid and kynurenine derivatives for neuroprotection. *Trends Pharmacol. Sci. 21*, 149–154.
9. Stone, T. W. (2000) Inhibitors of the kynurenine pathway. *Eur. J. Med. Chem. 35*, 179–186.
10. van Berkel, W. J., Kamerbeek, N. M., and Fraaije, M. W. (2006) Flavoprotein monooxygenases, a diverse class of oxidative biocatalysts. *J. Biotechnol. 124*, 670–689.
11. Ballou, D. P. (1984) Flavoprotein Monooxygenases. In *Flavins and Flavoproteins* (Bray, R. C., Engel, P. C., and Mayhew, S. G., Eds.), pp 605−618, Walter de Gruyter, Berlin, Germany.
12. Ballou, D. P., Entsch, B., and Cole, L. J. (2005) Dynamics involved in catalysis by single-component and two-component flavin-dependent aromatic hydroxylases. *Biochem. Biophys. Res. Commun. 338*, 590–598.
13. Husain, M., and Massey, V. (1979) Kinetic studies on the reaction of p-hydroxybenzoate hydroxylase. Agreement of steady state and rapid reaction data. *J. Biol. Chem. 254*, 6657–6666.
14. Palfey, B. A., Moran, G. R., Entsch, B., Ballou, D. P., and Massey, V. (1999) Substrate recognition by "password" in p-hydroxybenzoate hydroxylase. *Biochemistry 38*, 1153–1158.
15. Frederick, K. K., Ballou, D. P., and Palfey, B. A. (2001) Protein dynamics control proton transfers to the substrate on the His72Asn mutant of p-hydroxybenzoate hydroxylase. *Biochemistry 40*, 3891–3899.
16. Entsch, B., Ballou, D. P., and Massey, V. (1976) Flavin-oxygen derivatives involved in hydroxylation by p-hydroxybenzoate hydroxylase. *J. Biol. Chem. 251*, 2550–2563.
17. Detmer, K., and Massey, V. (1985) Effect of substrate and pH on the oxidative half-reaction of phenol hydroxylase. *J. Biol. Chem. 260*, 5998–6005.
18. Wang, J., Ortiz-Maldonado, M., Entsch, B., Massey, V., Ballou, D., and Gatti, D. L. (2002) Protein and ligand dynamics in 4-hydroxybenzoate hydroxylase. *Proc. Natl. Acad. Sci. U.S.A. 99*, 608–613.
19. Breton, J., Avanzi, N., Magagnin, S., Covini, N., Magistrelli, G., Cozzi, L., and Isacchi, A. (2000) Functional characterization and mechanism of action of recombinant human kynurenine 3-hydroxylase. *Eur. J. Biochem. 267*, 1092–1099.
20. Nishimoto, Y., Takeuchi, F., and Shibata, Y. (1979) Purification of L-kynurenine 3-hydroxylase by affinity chromatography. *J. Chromatogr. 169*, 357–364.
21. Kurnasov, O., Goral, V., Colabroy, K., Gerdes, S., Anantha, S., Osterman, A., and Begley, T. P. (2003) NAD biosynthesis: Identification of the tryptophan to quinolinate pathway in bacteria. *Chem. Biol. 10*, 1195–1204.
22. Crozier, K. R., and Moran, G. R. (2007) Heterologous expression and purification of kynurenine-3-monooxygenase from *Pseudomonas fluorescens* strain 17400. *Protein Expression Purif. 51*, 324–333.
23. Gawandi, V. B., Liskey, D., Lima, S., and Phillips, R. S. (2004) Reaction of *Pseudomonas fluorescens* kynureninase with β-benzoyl-L-alanine: Detection of a new reaction intermediate and a change in rate-determining step. *Biochemistry 43*, 3230–3237.
24. Massey, V. (1990) A Simple Method for the Determination of Redox Potentials. In *Flavins and flavoproteins* (Curti, B., Ronchi, S., and Zanetti, G., Eds.) pp 59−66, Walter de Gruyter & Co., New York.
25. Strickland, S., Palmer, G., and Massey, V. (1975) Determination of dissociation constants and specific rate constants of enzyme-substrate (or protein-ligand) interactions from rapid reaction kinetic data. *J. Biol. Chem. 250*, 4048–4052.
26. Jadan, A. P., van Berkel, W. J., Golovleva, L. A., and Golovlev, E. L. (2001) Purification and properties of p-hydroxybenzoate hydroxylases from *Rhodococcus* strains. *Biochemistry (Moscow, Russ., Fed.) 66*, 898–903.
27. Shoun, H., Arima, K., and Beppu, T. (1983) Inhibition of p-hydroxybenzoate hydroxylase by anions: Possible existence of two anion-binding sites in the site for reduced nicotinamide adenine dinucleotide phosphate. *J. Biochem. 93*, 169–176.
28. Detmer, K., and Massey, V. (1984) Effect of monovalent anions on the mechanism of phenol hydroxylase. *J. Biol. Chem. 259*, 11265–11272.
29. Howell, L. G., Spector, T., and Massey, V. (1972) Purification and properties of p-hydroxybenzoate hydroxylase from *Pseudomonas fluorescens*. *J. Biol. Chem. 247*, 4340–4350.
30. Spector, T., and Massey, V. (1972) Studies on the effector specificity of p-hydroxybenzoate hydroxylase from *Pseudomonas fluorescens*. *J. Biol. Chem. 247*, 4679–4687.
31. Spector, T., and Massey, V. (1972) p-Hydroxybenzoate hydroxylase from *Pseudomonas fluorescens*. Evidence for an oxygenated flavin intermediate. *J. Biol. Chem. 247*, 5632–5636.
32. Powlowski, J., Massey, V., and Ballou, D. P. (1989) Reactions of anthranilate hydroxylase with salicylate, a nonhydroxylated substrate analogue. Steady state and rapid reaction kinetics. *J. Biol. Chem. 264*, 5606–5612.
33. Giordani, A., Corti, L., Cini, M., Bormetti, R., Marconi, M., Veneroni, O., Speciale, C., and Varasi, M. (1996) Enantiospecific synthesis and in vitro activity of selective inhibitors of rat brain kynureninase and kynurenine-3-hydroxylase. *Adv. Exp. Med. Biol. 398*, 531–534.
34. Maeda-Yorita, K., and Massey, V. (1993) On the reaction mechanism of phenol hydroxylase. New information obtained by correlation of fluorescence and absorbance stopped flow studies. *J. Biol. Chem. 268*, 4134–4144.
35. Gatti, D. L., Palfey, B. A., Lah, M. S., Entsch, B., Massey, V., Ballou, D. P., and Ludwig, M. L. (1994) The mobile flavin of 4-OH benzoate hydroxylase. *Science 266*, 110–114.

36. Moran, G. R., Entsch, B., Palfey, B. A., and Ballou, D. P. (1999) Mechanistic insights into p-hydroxybenzoate hydroxylase from studies of the mutant Ser212Ala. *Biochemistry 38*, 6292–6299.
37. Palfey, B. A., Entsch, B., Ballou, D. P., and Massey, V. (1994) Changes in the catalytic properties of p-hydroxybenzoate hydroxylase caused by the mutation Asn300Asp. *Biochemistry 33*, 1545–1554.
38. The American Heart Association (2008) Heart Disease and Stroke Statistics 2008.
39. Carpenedo, R., Meli, E., Peruginelli, F., Pellegrini-Giampietro, D. E., and Moroni, F. (2002) Kynurenine 3-mono-oxygenase inhibitors attenuate post-ischemic neuronal death in organotypic hippocampal slice cultures. *J. Neurochem. 82*, 1465–1471.
40. Guidetti, P., Reddy, P. H., Tagle, D. A., and Schwarcz, R. (2000) Early kynurenergic impairment in Huntington's disease and in a transgenic animal model. *Neurosci. Lett. 283*, 233–235.
41. Moroni, F., Cozzi, A., Carpendo, R., Cipriani, G., Veneroni, O., and Izzo, E. (2005) Kynurenine 3-mono-oxygenase inhibitors reduce glutamate concentration in the extracellular spaces of the basal ganglia but not in those of the cortex or hippocampus. *Neuropharmacology 48*, 788–795.
42. Schwarcz, R., and Pellicciari, R. (2002) Manipulation of brain kynurenines: Glial targets, neuronal effects, and clinical opportunities. *J. Pharmacol. Exp. Ther. 303*, 1–10.
43. Cozzi, A., Carpenedo, R., and Moroni, F. (1999) Kynurenine hydroxylase inhibitors reduce ischemic brain damage: Studies with (m-nitrobenzoyl)-alanine (mNBA) and 3,4-dimethoxy-[N-4-(nitrophenyl)thiazol-2yl]-benzenesulfonamide (Ro 61-8048) in models of focal or global brain ischemia. *J. Cereb. Blood Flow Metab. 19*, 771–777.
44. Luthman, J. (2000) The kynurenine pathway of tryptophan degradation as a target for neuroprotective therapies. *Amino Acids 19*, 273–274.
45. Colabroy, K. L., and Begley, T. P. (2005) The pyridine ring of NAD is formed by a nonenzymatic pericyclic reaction. *J. Am. Chem. Soc. 127*, 840–841.
46. Enroth, C., Neujahr, H., Schneider, G., and Lindqvist, Y. (1998) The crystal structure of phenol hydroxylase in complex with FAD and phenol provides evidence for a concerted conformational change in the enzyme and its cofactor during catalysis. *Structure 6*, 605–617.
47. Peelen, S., Rietjens, I. M. C. M., Boersma, M. G., and Vervoort, J. (1995) Conversion of phenol derivatives to hydroxylated products by phenol hydroxylase from *Trichosporon cutaneum*: A comparison of regioselectivity and rate of conversion with calculated molecular orbital substrate characteristics. *Eur. J. Biochem. 227*, 284–291.
48. Hiromoto, T., Fujiwara, S., Hosokawa, K., and Yamaguchi, H. (2006) Crystal structure of 3-hydroxybenzoate hydroxylase from *Comamonas testosteroni* has a large tunnel for substrate and oxygen access to the active site. *J. Mol. Biol. 364*, 878–896.
49. Palfey, B. A., Ballou, D. P., and Massey, V. (1997) Flavin conformational changes in the catalytic cycle of p-hydroxybenzoate hydroxylase substituted with 6-azido- and 6-aminoflavin adenine dinucleotide. *Biochemistry 36*, 15713–15723.
50. Moran, G. R., Entsch, B., Palfey, B. A., and Ballou, D. P. (1996) Evidence for flavin movement in the function of p-hydroxybenzoate hydroxylase from studies of the mutant Arg220Lys. *Biochemistry 35*, 9278–9285.
51. Moran, G. R., Entsch, B., Palfey, B. A., and Ballou, D. P. (1997) Electrostatic effects on substrate activation in para-hydroxybenzoate hydroxylase: Studies of the mutant lysine 297 methionine. *Biochemistry 36*, 7548–7556.
52. Ortiz-Maldonado, M., Entsch, B., and Ballou, D. P. (2003) Conformational changes combined with charge-transfer interactions are essential for reduction in catalysis by p-hydroxybenzoate hydroxylase. *Biochemistry 42*, 11234–11242.
53. Palfey, B. A., Basu, R., Frederick, K. K., Entsch, B., and Ballou, D. P. (2002) Role of protein flexibility in the catalytic cycle of p-hydroxybenzoate hydroxylase elucidated by the Pro293Ser mutant. *Biochemistry 41*, 8438–8446.
54. Massey, V. (1994) Activation of molecular oxygen by flavins and flavoproteins. *J. Biol. Chem. 269*, 22459–22462.

BI8010434